Supplementary Material for:

Three-Dimensional Multilevel Nanoporous $NiCoO_2$/Ni Hybrid for Highly Reversible Electrochemical Energy Storage

Binbin Liu,[a] Jiagang Hou,[b] Tingting Zhang,[a] Caixia Xu,[a]* and Hong Liu[ac]*

[a]*Collaborative Innovation Center of Technology and Equipement for Biological Diagnosis and Therapy in Universities of Shandong, Institute for Advanced Interdisciplinary Research (iAIR), University of Jinan, Jinan, 250022, P. R. China*

[b]*Qilu University of Technology (Shandong Academy of Sciences)*

Jinan 250353, Shandong Province, P. R. China

[c]*State Key Laboratory of Crystal Materials, Shandong University*

Jinan 250100, P. R. China

Fax: +86-531-82767033; Tel: +86-531-82767033

E-mail: chm_xucx@ujn.edu.cn; hongliu@sdu.edu.cn

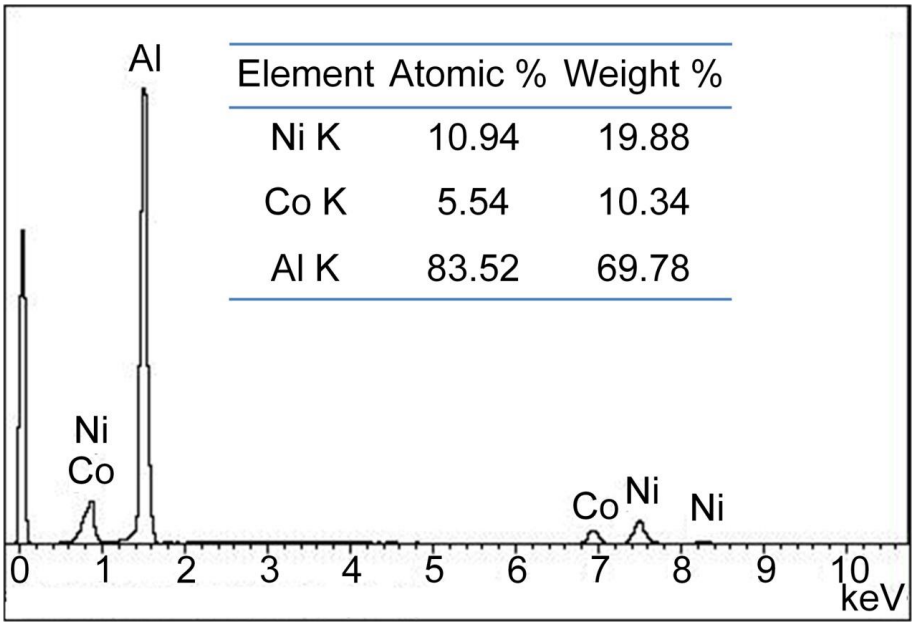

Element	Atomic %	Weight %
Ni K	10.94	19.88
Co K	5.54	10.34
Al K	83.52	69.78

Fig. S1. EDS data of the $Ni_{10}Co_5Al_{85}$ precursor alloy.

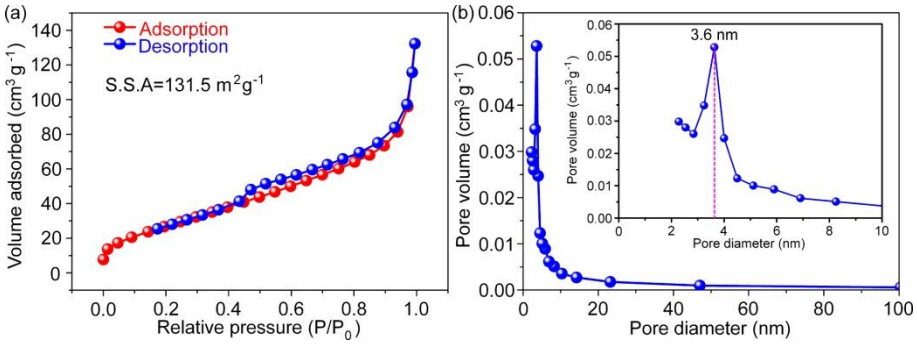

Fig. S2. The N_2 adsorption-desorption isotherms and BJH pore size distribution curves of the $NiCoO_2$/Ni hybrid after etching the $Ni_{10}Co_5Al_{85}$ alloy.

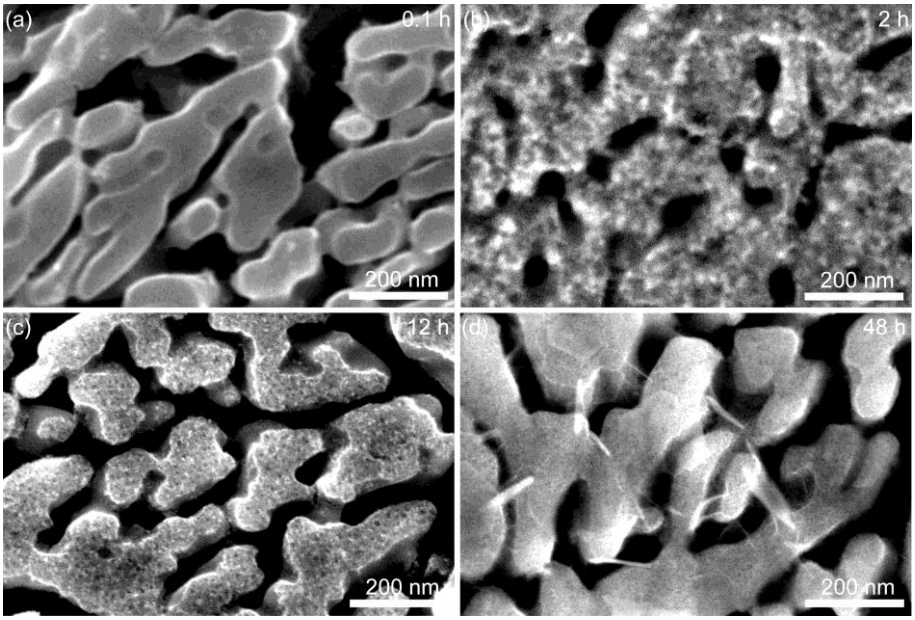

Fig. S3. SEM images of the dealloyed samples at different corrosion times for (a) 0.1 h, (b) 2 h, (c) 12 h, and (d) 48 h, respectively.

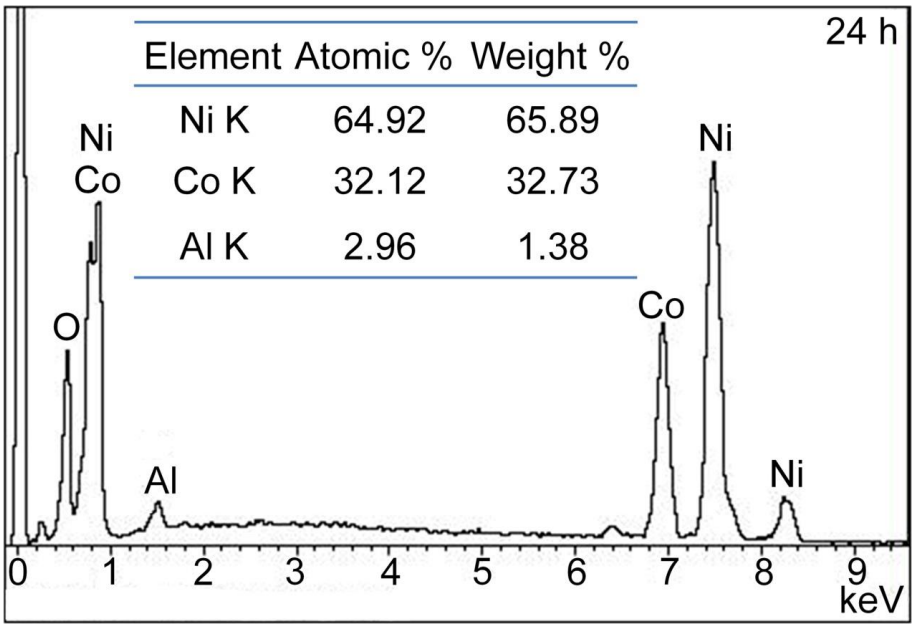

Fig. S4. EDS data of the $NiCoO_2$/Ni product upon dealloying for 24 h.

Time (h)	Ni K (Atomic/Weight %)	Co K (Atomic/Weight %)	Al K (Atomic/Weight %)
0.1	54.26/60.57	26.25/29.42	19.49/10.01
2	56.91/61.07	30.21/32.56	12.88/6.37
12	58.72/62.58	29.65/31.72	11.63/5.70
24	64.92/65.89	32.12/32.73	2.96/1.38
48	65.08/65.93	32.30/32.85	2.62/1.22

Fig. S5. EDS data of the products with different dealloying times.

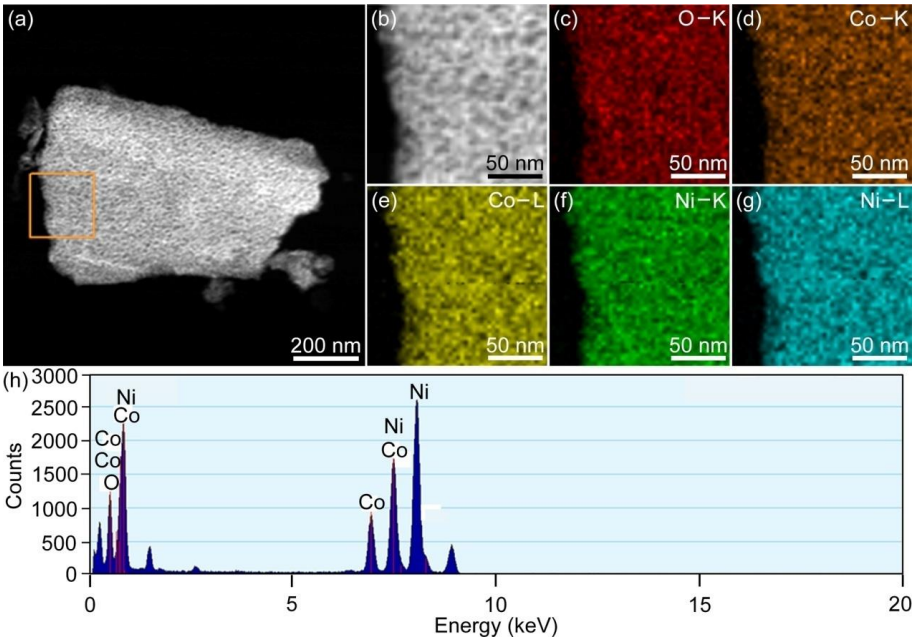

Fig. S6. EDS elemental mapping of the $NiCoO_2$/Ni hybrid.

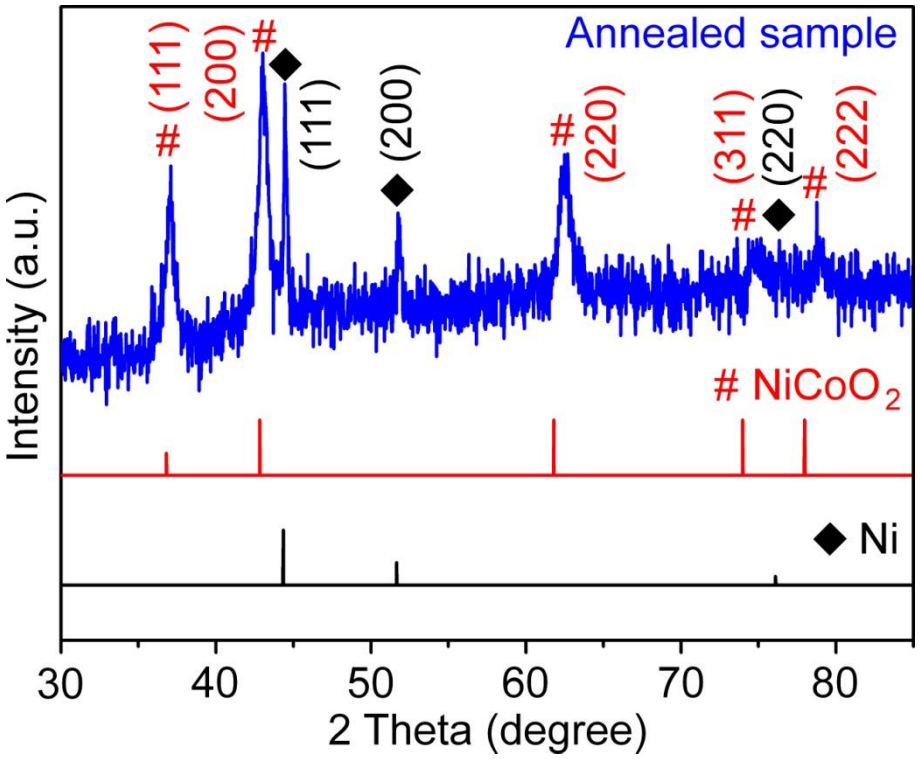

Fig. S7. XRD pattern of the dealloyed product annealed at 600 ºC for 2 h. The standard patterns of $NiCoO_2$ (JCPDS 10-0188) and Ni (JCPDS 65-0380) are included for comparison.

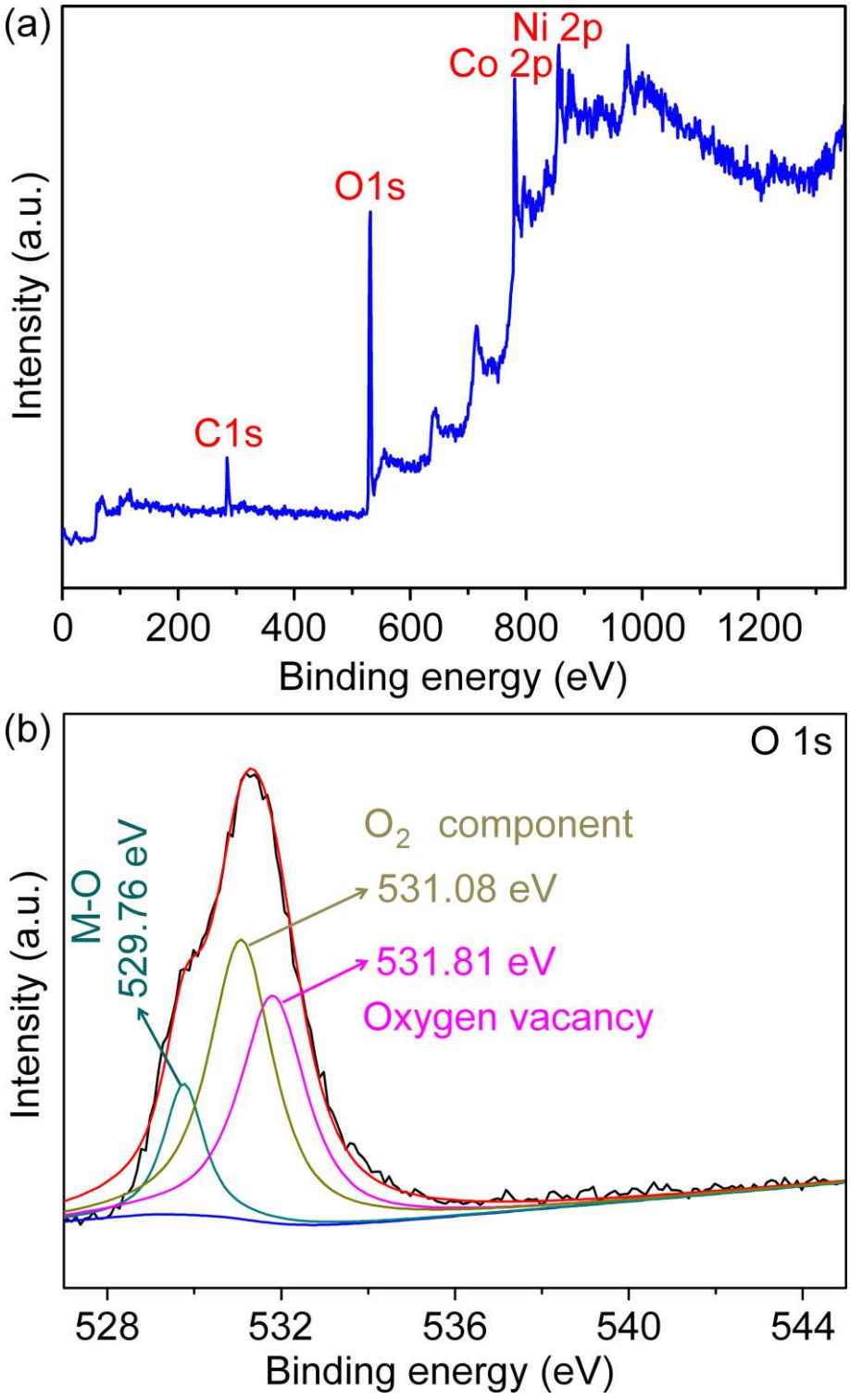

Fig. S8. (a) XPS data for $NiCoO_2$/Ni, (b) high-resolution XPS for the O 1s in $NiCoO_2$/Ni hybrid.

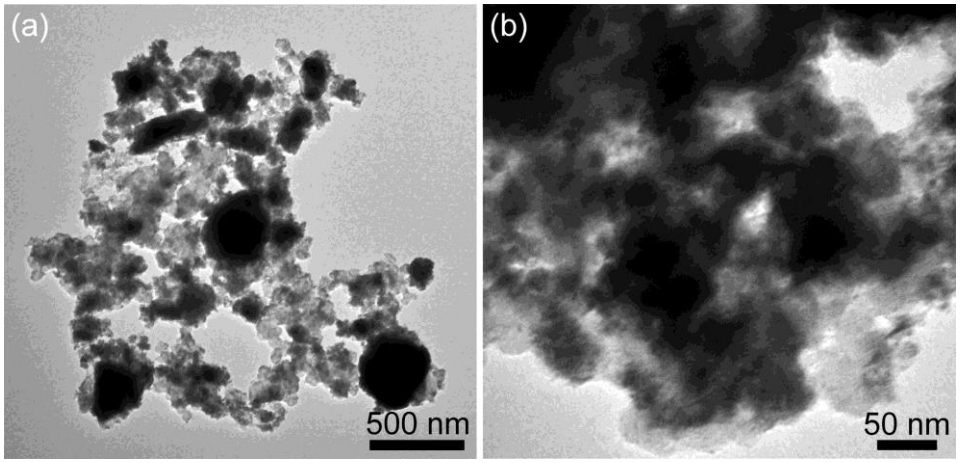

Fig. S9. TEM images of the $NiCoO_2$/Ni hybrid after 5000 CV cycles.

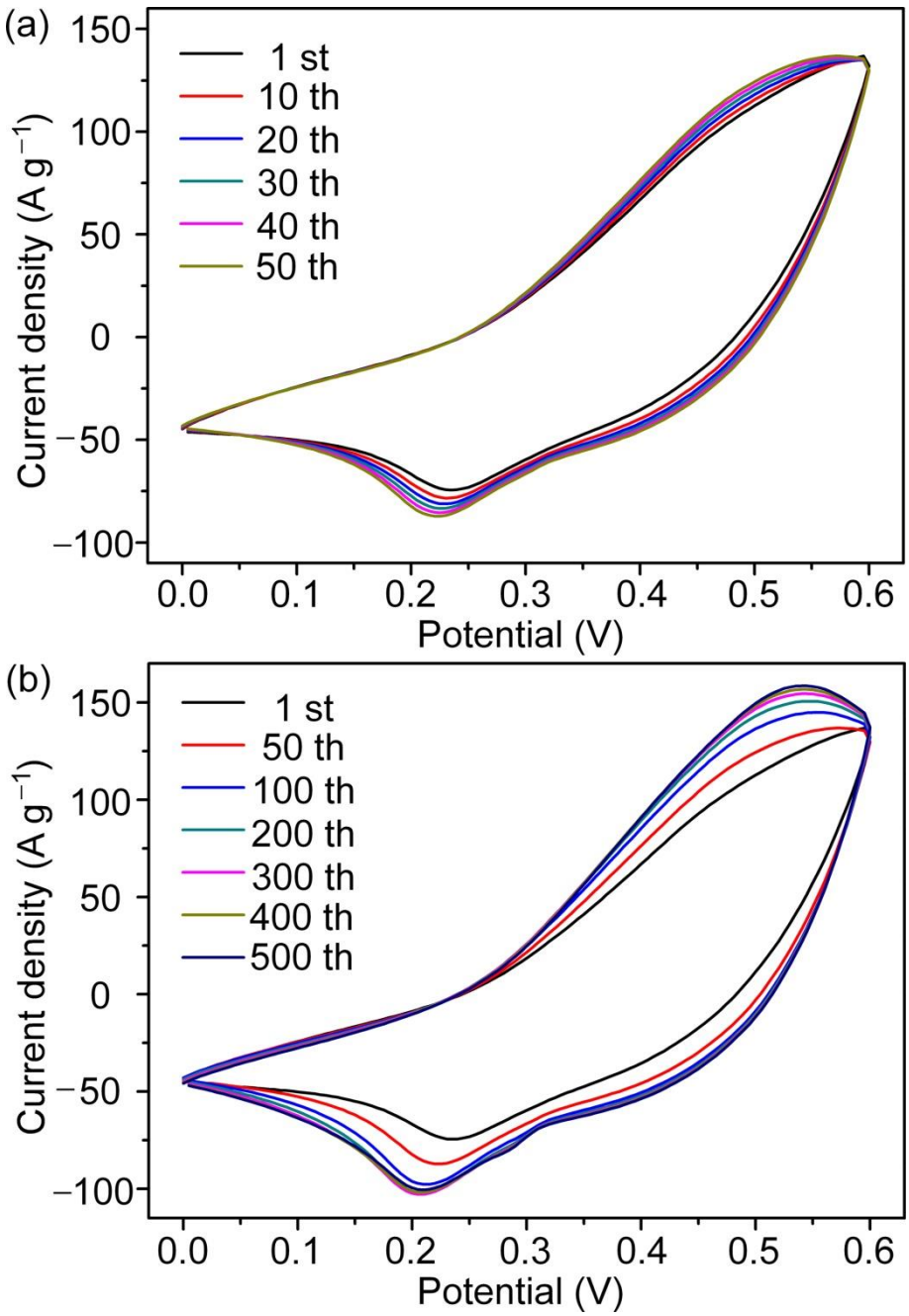

Fig. S10. (a&b) CV curves (50 mV s^{-1}) of the $NiCoO_2$/Ni electrode with different cycles as indicated.

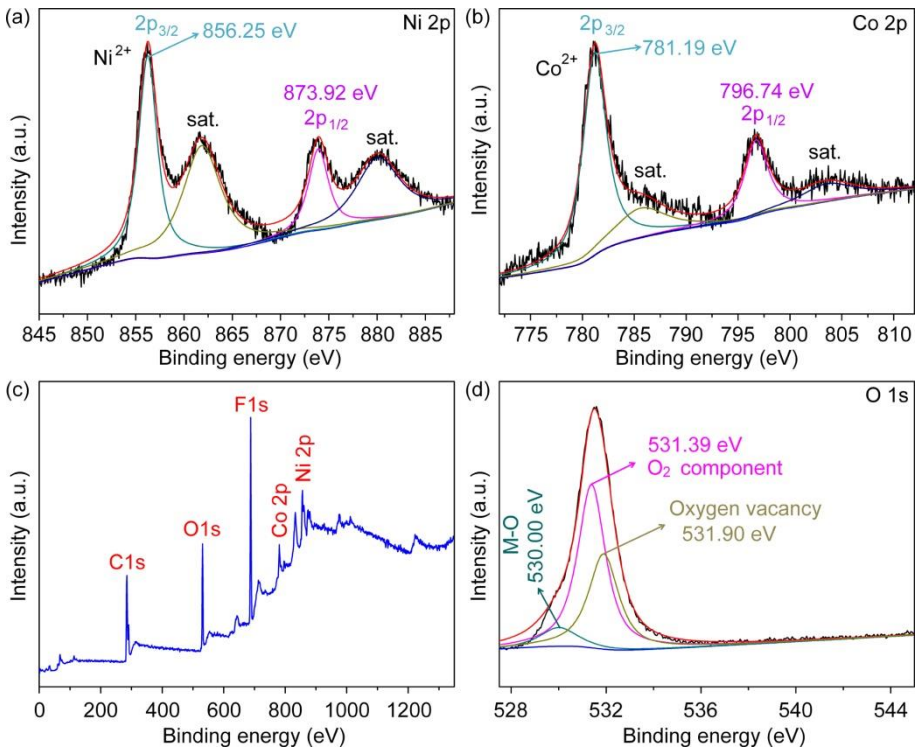

Fig. S11. XPS date of the $NiCoO_2$/Ni hybrid after 200 CV cycles.

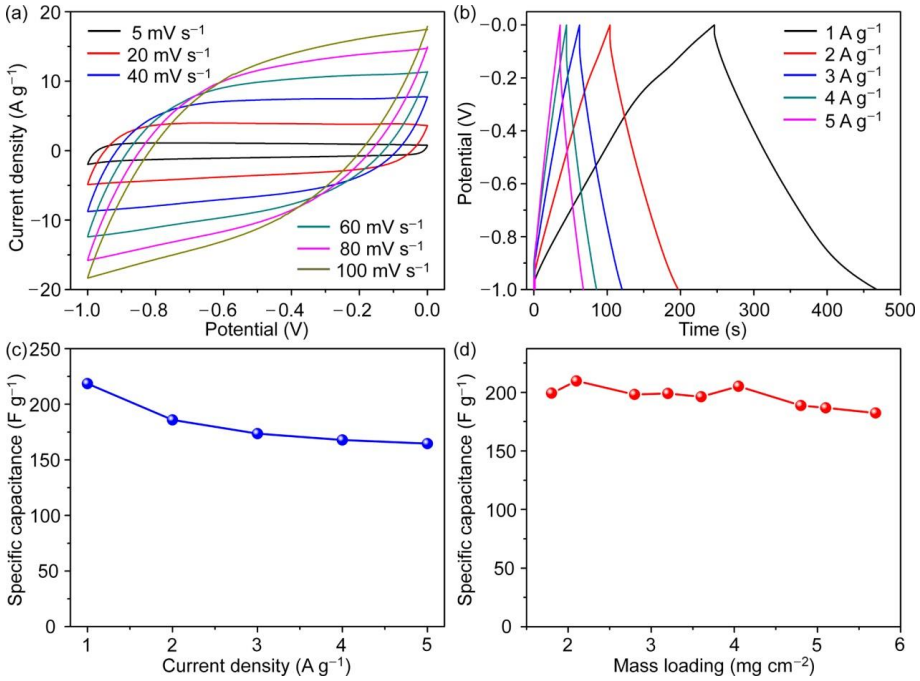

Fig. S12. (a) CV curves, (b) GCD curves, (c) specific capacitance at different current densities of the AC anode, (d) specific capacitance of different electrodes with various mass loading.

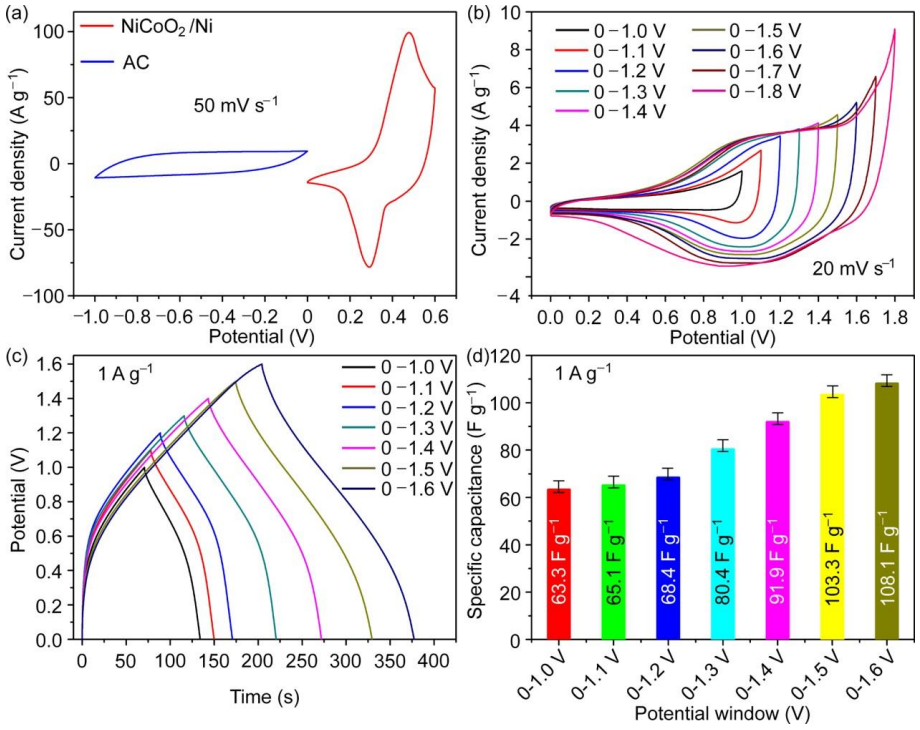

Fig. S13. (a) CV curves of AC and $NiCoO_2$/Ni electrodes, (b) CV curves, (c) GCD curves of the ASC at different potential windows, (d) Specific capacitance at different potential windows.